Scalar Limitations of Diffractive Optical Elements

Eric G. Johnson and Diane Hochmuth
Teledyne Brown Engineering
Sensor Systems Department
300 Sparkman Drive
Huntsville, Alabama 35807

M.G. Moharam and Drew Pommet
CREOL, University of Central Florida
Orlando, Florida

ABSTRACT

In this paper, scalar limitations of diffractive optic components are investigated using coupled wave analyses. Results are presented for linear phase gratings and fanout devices. In addition, a parametric curve is given which correlates feature size with scalar performance.

1. INTRODUCTION

Diffractive Optical Elements (DOE) are utilized in optical computing architectures, fiber optic systems, imaging cameras and numerous optoelectronic devices[1]. The major advantages are realized in coherent systems, due to the inherent chromatic behavior of these elements. Since DOE's are fabricated using standard photolithographic equipment, the feature sizes can be on the order of wavelengths. However, when the features are a few wavelengths, as is the case for fast microlens arrays, the scalar assumptions are no longer valid. To address this issue, exact electromagnetic modeling must be incorporated in the design process.

In this paper, the rigorous coupled wave formulation is implemented to determine where the separation is between the scalar theory and exact formulations. First, an analysis is presented for a discrete linear phase grating to demonstrate the polarization and coupling effects as a function of period size. Second, a Dammann fanout device is analyzed to demonstrate the effects on beam uniformity as a function of both polarization and period size. Third, an attempt is made to characterize the effect of feature sizes characteristic in multilevel structures.

2. THEORY

Diffractive optic components rely on phase perturbations in the transmitted wavefront to diffract the light. Quite often this is performed using 2π structures etched into a glass substrate using standard photolithographic techniques. Figure 1 illustrates a collapsed diffractive lens. This plate can be viewed as a series of zones diffracting energy into a prescribed diffraction order, as the zones move away from the center they become smaller since they are required to diffract energy through larger angles. Therefore, the smaller zones can be modeled as a dielectric grating since adjacent zone dimensions do not significantly change. For a multilevel diffractive optic, the -1 diffraction efficiency can be approximated using scalar diffraction theory as follows:

$$DE_{-1}=T^2\left(\frac{\sin\left(\frac{\pi}{N}\right)}{\left(\frac{\pi}{N}\right)}\right)^2$$

(1)

where, T represents the transmission coefficient squared and N is the number of phase levels used to approximate the profile. To determine the diffraction angle for a given zone, the grating equation is employed

$$\sin \theta_{-1} = \frac{\lambda}{(n)(\text{period})} \tag{2}$$

where λ is the wavelength and n is the index of refraction. The period is the zone size which is modeled as a grating unit cell. Another side effect of the small zones is that the scalar, or paraxial, assumptions associated with diffraction efficiencies are no longer valid and more robust techniques are required. Therefore, Maxwell's equations must be implemented to accurately model the polarization sensitivities and resonances present in small structures. Although numerous formulations exist under diverse titles, the majority require solutions to a system of differential or integral equations. The most common technique used for dielectric grating profiles is the coupled-mode approach, wherein a system of differential equations is solved[2]. The first step is to expand the fields in the incident and transmitted regions in terms of a common basis set representational of the floquet modes

$$\vec{E}_1(x,y) = \vec{E}_{inc}(x,y) + \sum_n \vec{R}_n e^{j(\alpha_n x + \beta_n^1 y)}$$

$$\vec{E}_2(x,y) = \sum_n \vec{T}_n e^{j(\alpha_n x + \beta_n^2 y)} \tag{3}$$

Since the modulated region is a multilayer structure of air/dielectric rectangles, it is expanded in the same basis set. This yields the following set of equations for the fields and modulated index:

$$E(x,y) = \sum_n E_n(y) e^{j\alpha_n x}$$

$$H(x,y) = \sum_n H_n(y) e^{j\alpha_n x}$$

$$\varepsilon(x,y) = \sum_m a_m(y) e^{j\alpha_m x}$$

$$\frac{1}{\varepsilon(x,y)} = \sum_m b_m(y) e^{j\alpha_m x} \tag{4}$$

operating on these field components with the curl equations, a set of coupled differential equations is formed for the modulated region

$$\frac{d}{dy} \begin{bmatrix} E_n \\ H_n \end{bmatrix} = \begin{bmatrix} A_{nm} & B_{nm} \\ C_{nm} & D_{nm} \end{bmatrix} \begin{bmatrix} E_m \\ H_m \end{bmatrix} \tag{5}$$

Then, an eigenvalue/vector computation is performed to derive the solution set for each sublayer.

$$E(x,y) = \sum_n \sum_m C_m W_{nm} e^{(\lambda_m y + j\alpha_n x)}$$

$$H(x,y) = \sum_n \sum_m C_m W_{nm} e^{(\lambda_m y + j\alpha_n x)} \tag{6}$$

After this is accomplished, the fields are matched to the incident and transmitted regions for computing the R_n and T_n coefficients. These are then used to compute the diffraction efficiencies and field values at any desired point.

3. NUMERICAL RESULTS

3.1 LINEAR PHASE GRATING

In order to determine where the scalar theory breaks down with a linear phase grating, a multistep grating was modeled using the coupled wave theory. Figure 2 illustrates an eight phase level structure with the polarizations defined as E and H, where E is parallel to the grooves and H is when the E lies in the plane of incidence. The computed diffraction efficiency for the -1 order is illustrated in Figure 3 as a function of period size and index of refraction. As can be expected for periods approximately a few wavelengths in size, scalar theory breaks down; whereas, for periods greater than 20 wavelengths the performance is close to scalar. Moreover, as the index is increased the scalar approximation is realized at smaller periods.

As was previously mentioned, the primary mechanism in the diffraction process is the phase modulation; therefore, to diffract the energy into the -1 order, the phase should be a stepwise linear approximation across the unit cell. To verify that the phase was linear after immediately passing through the profile, a scan of the phase was computed for both large and small period sizes. Figures 4 and 5 represent the results for both polarization states at period sizes of 2 and 20 wavelengths respectively. The small period demonstrated a complex phase profile for both E and H modes which signified a departure from scalar theory. In the 20 wavelength case, both polarizations demonstrated a well defined linear phase function close to the scalar approximation.

3.2 FANOUT DEVICES

Another area of interest is in fanout phase grating structures. Although numerous techniques exist for beam splitting, one of the most common is a Dammann grating as illustrated in Figure 6. Due to the thickness of the grating structure, the transmitted light assumes a 0 or π phase shift which is then used to diffract the light into a predetermined number of diffracted orders with uniform intensity[3]. However, as the number of desired spots is increased, so is the number of transition points in the grating profile. The increase in the number of transition points forces smaller features in the grating design which must be investigated using rigorous modeling techniques.

As an example, a five beam Dammann device was analyzed as a function of feature size. Figure 7 illustrates the unit cell which was designed in glass (n=1.5). This design was optimized using a steepest descent algorithm with scalar assumptions for a spot uniformity of less than 1% and an average DE of 14.9%. Uniformity is defined as follows:

$$\%\text{Unif} = 100 \times \left(\frac{P_{max} - P_{min}}{P_{avg}} \right)$$

(7)

Figures 8 and 9 illustrate the spot uniformity and average DE as a function of period size for the 5 beam array. These results demonstrated polarization sensitivities and an unacceptable beam uniformity for period sizes up to 50 wavelengths. Therefore, to obtain acceptable performance out of a Dammann device, the period must be hundreds of wavelengths when there are small features.

3.3 FEATURE SIZE STUDY

Many concerns exist as to when scalar theory actually breaks down and how do you design around this phenomena. Additional studies have implicated that it is not the period size, but the actual feature size relative to a wavelength that causes the separation from scalar. In an attempt to verify this effect, numerous analyses were performed on a biphase-level structure

with alternate fill factors as illustrated in Figure 10. Seven fill factors were analyzed: 0.9375, 0.875, 0.75, 0.5, 0.25, 0.125, and 0.0625. Since most of the scattering occurs at the corners of the structure, only the E mode was analyzed with the coupled wave theory. The -1 order diffraction efficiency was compared to Fourier theory as a ratio. Figure 11 illustrates the result for an index of refraction of 1.5. The implications of these results signify extreme fluctuations in the DE as a function of feature size and as the index of refraction is increased, the effect is diminished.

4. CONCLUSIONS

In this study, the rigorous coupled wave approach was used to investigate the scalar limitations of diffractive optics. This analysis verified that coupling effects influence the diffraction efficiencies of the multistep phase gratings. Additionally, polarization sensitivities were observed for Dammann gratings with small features. Considering these findings, rigorous analyses must be performed when designing DOE's with feature sizes on the order of a wavelength. Areas of additional studies include the dispersive effects of multiphase structures, and angle of incidence effects. Further developments in the analytical tools are also required to adequately predicts the three-dimensional diffraction of microlens structures. Moreover, alternate formulations from the coupled mode approach are needed due to the increased ode coupling of a three-dimensional structure.

5. ACKNOWLEDGEMENTS

The authors would like to thank Anthony Cook, Jeff Howard and Jo Knight of Teledyne Brown Engineering for assisting in this effort. Also, Alan Kathman for his continual technical support and motivation.

6. REFERENCES

1. Alan Kathman and Eric Johnson, "Binary Optics; New Diffractive Elements for the Designer's Tool Kit. Photonics Spectra,, pp. 125-132, September 1992."

2. Moharam, M. and Gaylord, T. "Diffractive Analysis of a Surface Relief Grating," JOSA A. , Vol. 72, pp. 1385-1392, Oct. 1982.

3. Krackhardt. U. and Streibl, N. "Design of Dammann-Gratings for Array Generation," Optics Communications., Vol. 28, pp. 1267-1275, Dec. 1989.
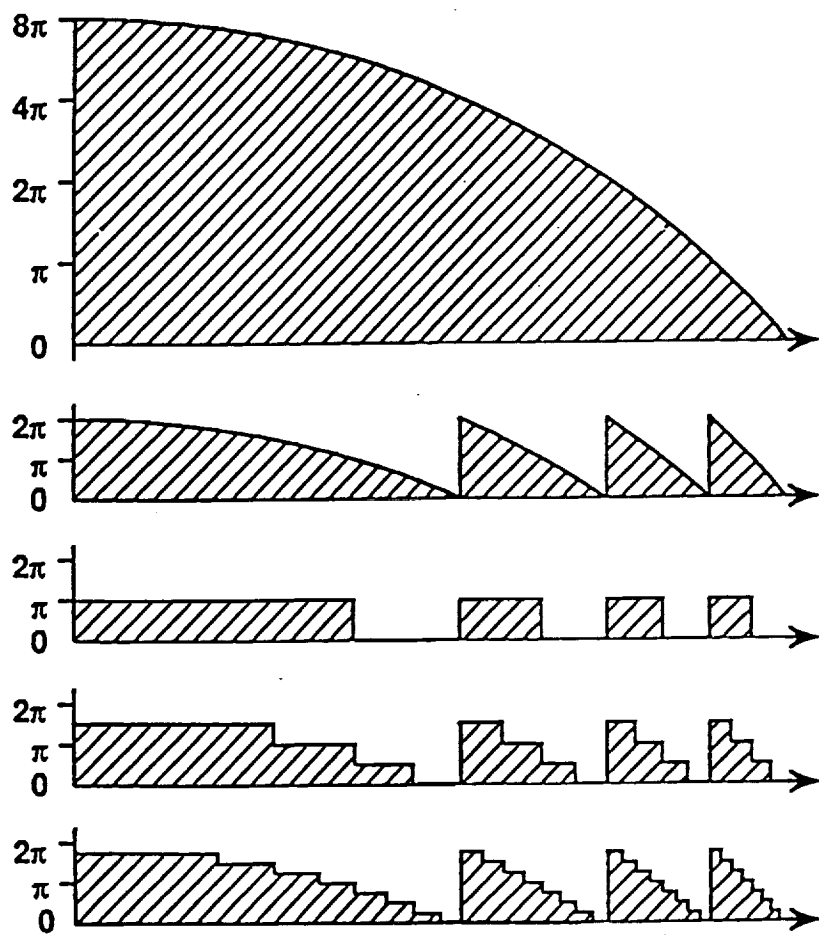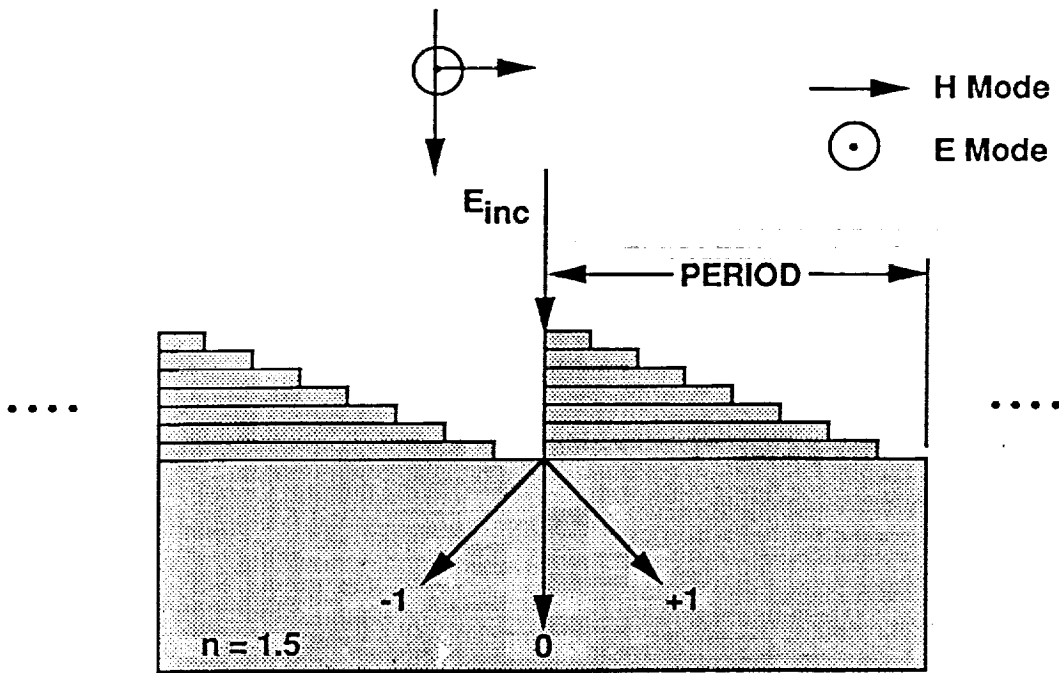
Figure 1. Diffractive collapsed-phase lens.

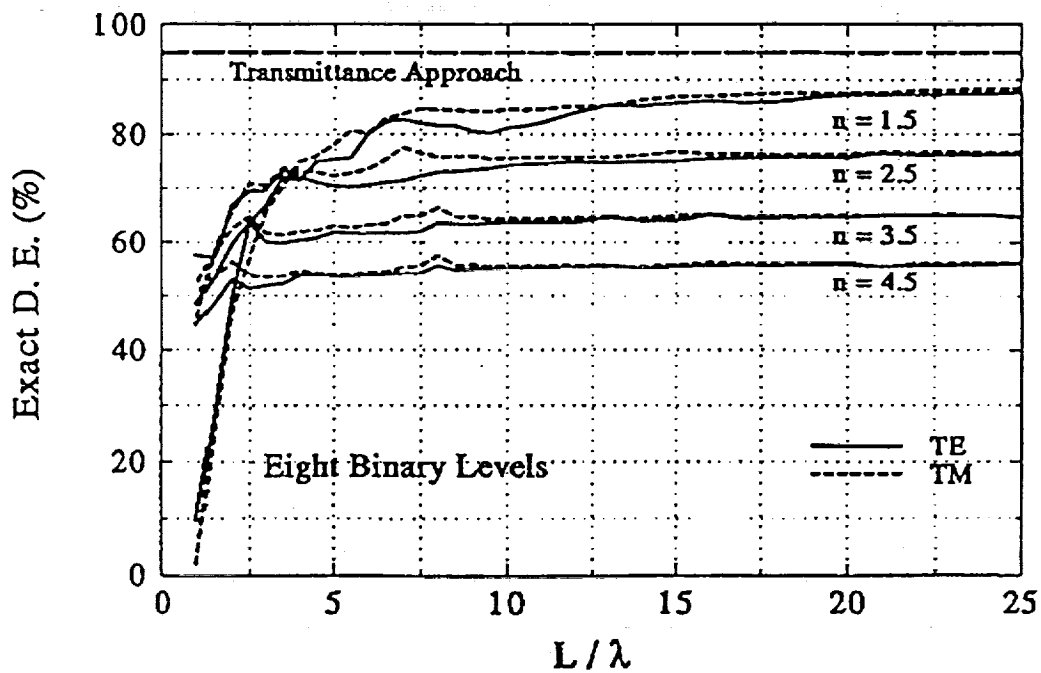Figure 2. Linear phase grating geometry.

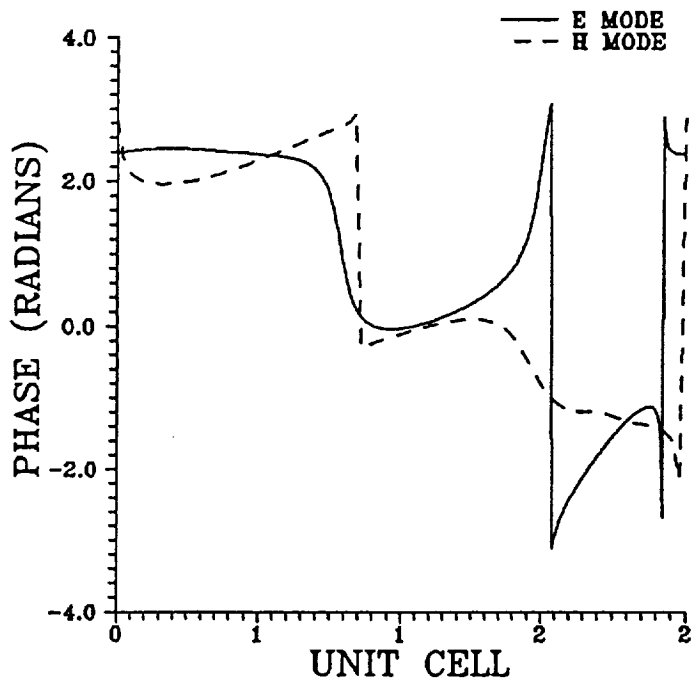Figure 3. -1 DE comparison for an eight phase level grating.

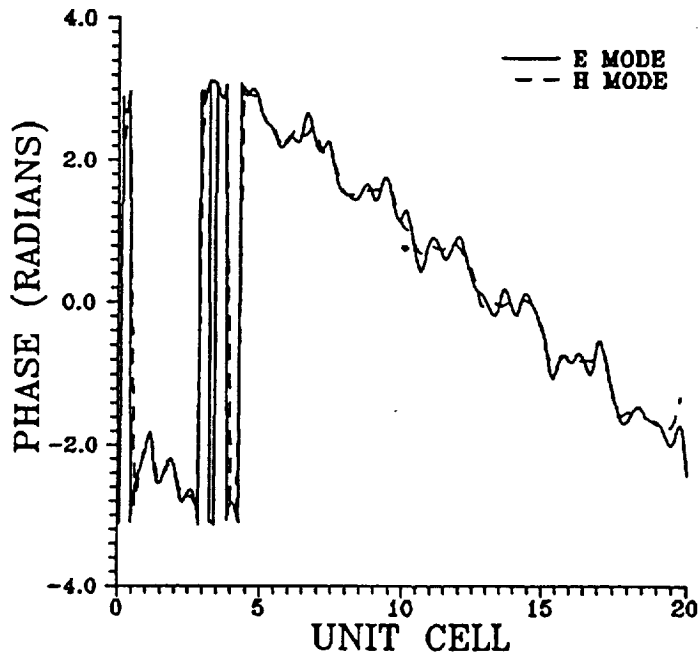Figure 4. Eight level phase computation for two wavelength
period.

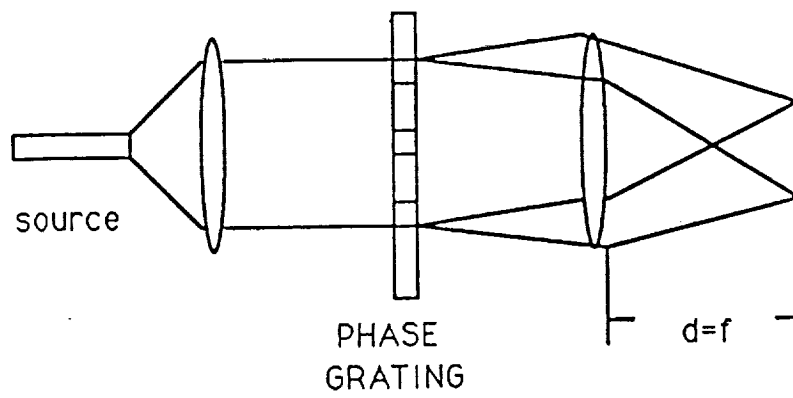Figure 5. Eight level phase computation for twenty wavelength
period.

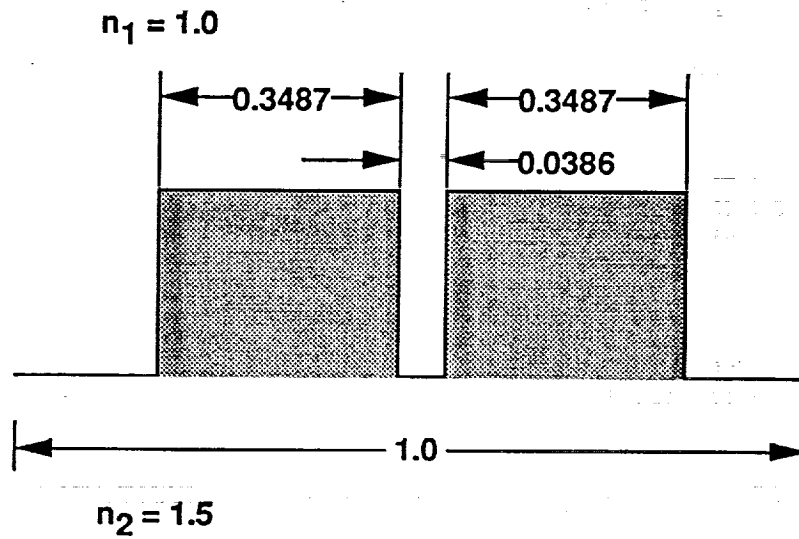Figure 6. Optical implementation of a Dammann grating.

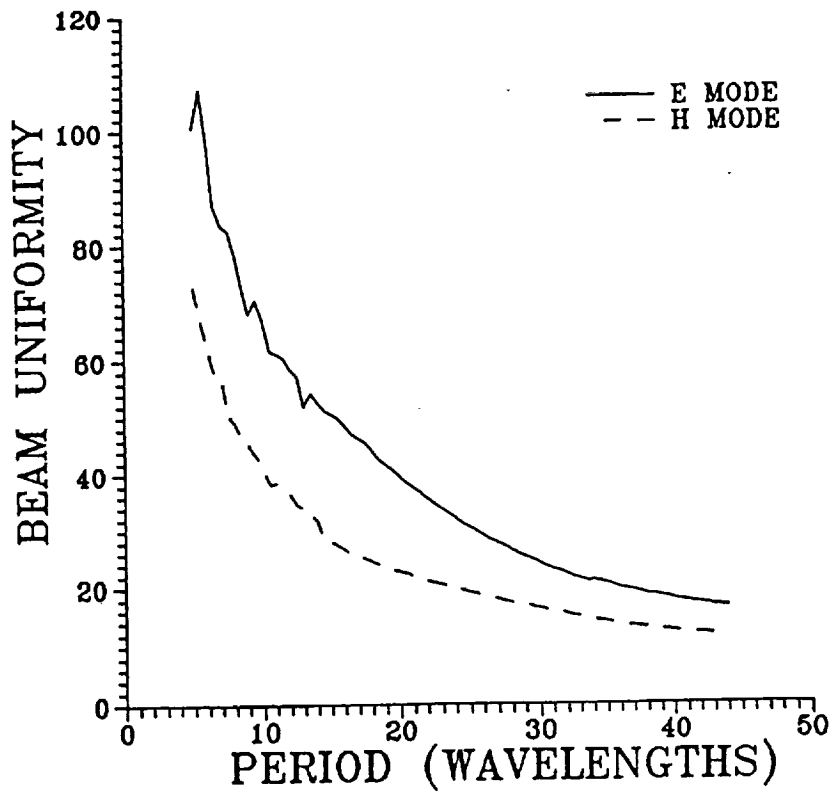Figure 7. Dammann 5 beam unit cell.

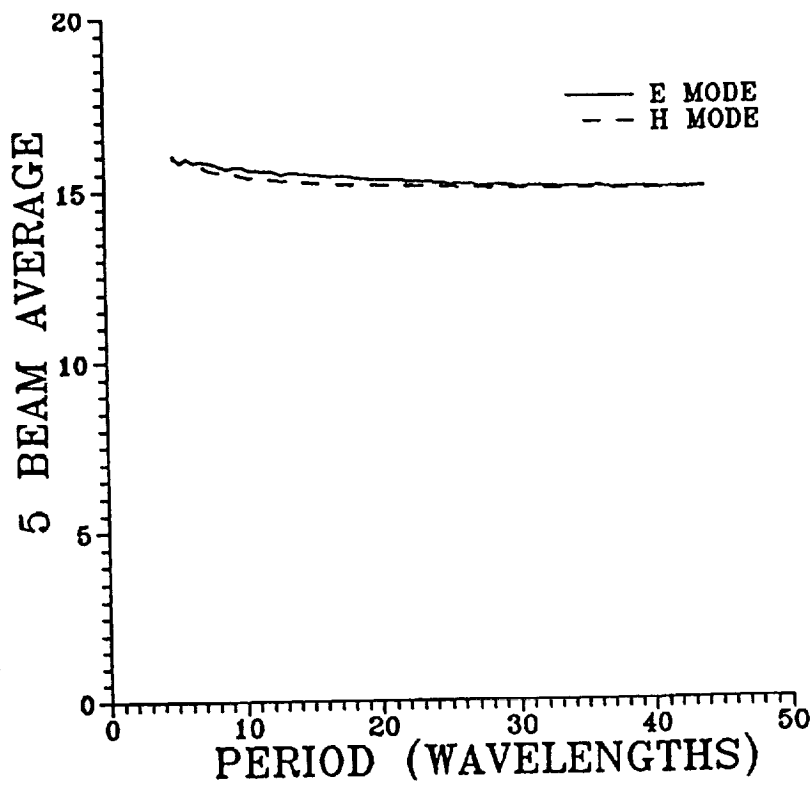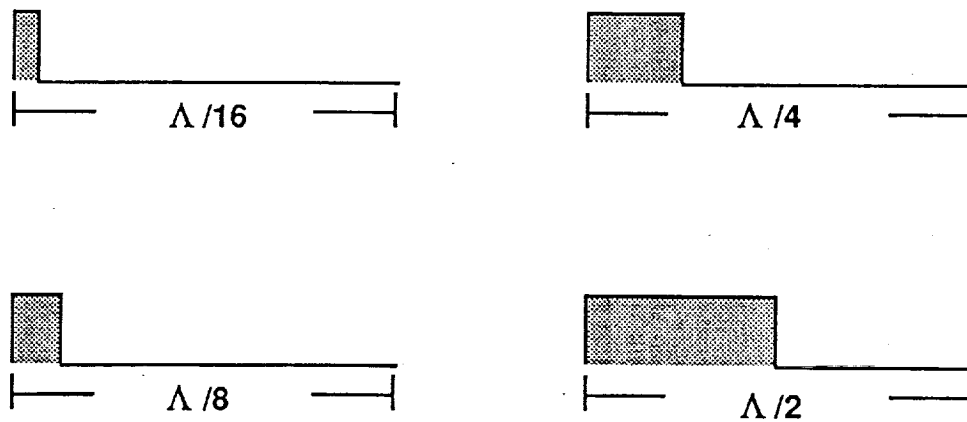Figure 8. Computed beam uniformity for a 5 beam Dammann device.

Figure 9. Computed average for a 5 beam Dammann device.
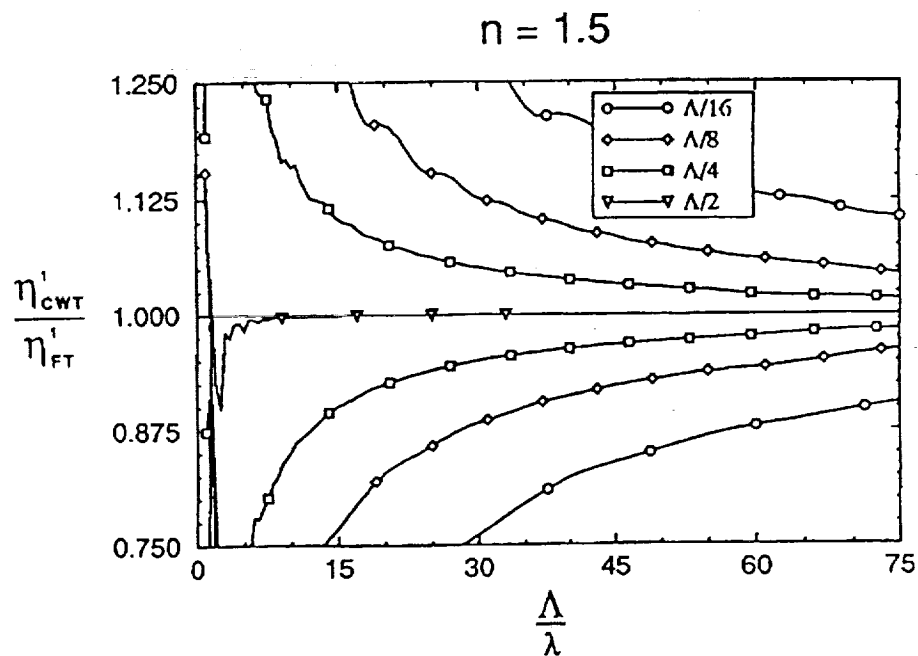
C-2

Figure 10. Fill factor geometry.

Figure 11. Exact and scalar comparisons for E mode as a function of feature size.
(fill factors > 0.5 are given in the lower half)